THE ROUGH-WALL TURBULENT BOUNDARY LAYER FROM THE HYDRAULICALLY SMOOTH TO THE FULLY ROUGH REGIME

Karen A. Flack
Department of Mechanical Engineering
United States Naval Acadmy
Annapolis, MD 21402 USA
flack@usna.edu

Michael P. Schultz
Department of Ocean Engineering and Naval Architecture
United States Naval Acadmy
Annapolis, MD 21402 USA
mschultz@usna.edu

ABSTRACT

Turbulence measurements for rough-wall boundary layers are presented and compared to those for a smooth wall. The rough-wall experiments were made on a three-dimensional, rough surface geometrically similar to the honed pipe roughness used in the study of Shockling, *et al.* (2006). The present work is unique in that it covers a wide Reynolds number range (Re_θ = 2180 - 27100), spanning the hydraulically smooth to the fully rough flow regimes for a single surface, while maintaining a roughness height that is a very small fraction of the boundary layer thickness. The mean velocity profiles for the rough and smooth walls show remarkable similarity in the outer layer using velocity-defect scaling. The Reynolds stresses and higher order turbulence statistics also show excellent agreement in the outer layer. The results lend strong support to the concept of outer layer similarity for rough walls in which there is a large separation between the roughness length scale and the largest turbulence scales in the flow.

INTRODUCTION

Understanding the effect of roughness on wall-bounded turbulence is of practical importance in the prediction of a wide range of industrial and geophysical flows. An extensive review of the literature on rough-wall boundary layers was given by Raupach, *et al.* (1991). An important conclusion of their work was that there is strong experimental evidence of outer layer similarity in the turbulence structure over smooth and rough walls outside the roughness sublayer. The roughness sublayer is the region directly above the roughness, extending about 5 roughness heights, in which the turbulent motions are directly influenced by the roughness length scales. Raupach, *et al.* (1991) noted that the wall similarity hypothesis is an extension of Townsend's (1976) concept of Reynolds number similarity for turbulent flows.

Since Raupach's review, the concept of wall similarity has come into question. Experimental studies of rough-wall boundary layers by Krogstad, *et al.* (1992), Tachie, *et al.* (2000), and Keirsbulck, *et al.* (2002) have all observed significant changes to the Reynolds stresses that extend well into the outer layer for flows over woven mesh and transverse bar roughness. Numerical simulations of turbulent channel flow by Leonardi, *et al.* (2003) and Bhaganagar, *et al.* (2004) also show that roughness effects can be observed in the outer layer. However, the recent experimental studies of Kunkel & Marusic (2006) and the present authors (Flack, *et al.* 2005) provide support for wall similarity in smooth- and rough-wall boundary layers in terms of both the mean flow and the Reynolds stresses. In a recent review, Jiménez (2004) states that the conflicting views regarding the validity of the wall similarity hypothesis may be due to the effect of the relative roughness, k/δ, on the flow.

The purpose of the present study was to critically assess its validity when the criteria for similarity are strictly adhered to. That is, the Reynolds number is sufficiently high and the roughness is small compared to the boundary layer thickness. It would seem that wall similarity for larger relative roughness cannot be expected if it does not hold true for the limiting case. In this study, the structure of the rough-wall boundary layers in terms of the mean flow, Reynolds stresses, and higher order turbulence statistics are compared with those for a smooth wall. The present work is unique in that it covers a wide Reynolds number range, spanning the hydraulically smooth to the fully rough flow regime for a single surface, while maintaining a roughness height that is a very small fraction of the boundary layer thickness.

EXPERIMENT

The experiments were conducted in the U.S. Naval Academy's large re-circulating water tunnel. The test section of the tunnel is 40 cm by 40 cm in cross-section and is 1.8 m in length with speeds from 0 – 8 m/s, as shown in figure 1. The current tests were run at six speeds within this range, producing a wide variation in Reynolds number (Re_θ = 2,180 - 27,100) as shown in table 1. Boundary layer

velocity measurements were obtained with a TSI FSA3500 two-component laser Doppler Velocimeter (LDV). The LDV consists of a four beam fiber optic probe that collects data in backscatter mode. A total of 40,000 random velocity measurements were obtained at 40 locations in the boundary layer. Two test plates were used in the current study. The smooth surface was made of cast acrylic. The rough surface was produced by scratching a cast acrylic plate coated with filled polyamide epoxy to produce diamond shaped grooves, similar to the surface of a honed pipe (Shockling, *et al.* 2006). The roughness was chosen to be a small fraction of the boundary layer thickness ($k_{rms}/\delta < 0.1\%$) and to cover the hydraulically smooth to fully-rough flow regimes for the range of velocities tested. The surface topography of the riugn surface is shown in figure 2a and the probability density function (*pdf*) for the surface roughness elevations is presented in figure 2b. The surface has a nearly Gaussian *pdf* with a root-mean-square height, k_{rms}, of 26.3 μm. The skewness of the *pdf* is -0.46 and the flatness is 3.59.

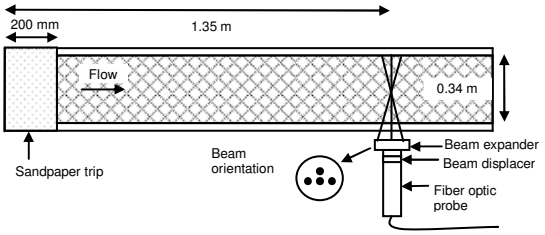

Figure 1. Experimental set-up.

Surface	U_e (ms^{-1})	Re_θ	U_τ (ms^{-1})	δ (mm)	δ^+	k_s^+	ΔU^+
Smooth	1.00	3,110	0.0405	29.0	1,150	--	--
Smooth	5.00	13,140	0.181	26.3	4,760	--	--
Rough	0.69	2,175	0.0295	29.2	843	2.3	0
Rough	1.00	3,175	0.0415	28.9	1,180	3.2	0.14
Rough	3.00	8,450	0.119	27.1	3,150	9.2	1.5
Rough	5.00	13,800	0.202	25.5	5,120	16	3.0
Rough	7.02	21,360	0.285	27.6	8,030	23	4.2
Rough	7.96	27,080	0.322	31.2	10,100	26	4.6

Table 1. Experimental test conditions.

The friction velocity, U_τ, for both the smooth and rough surfaces, are listed in table 1. For the smooth wall, the friction velocity was determined using the Clauser (1954) chart method, with log-law constants κ= 0.421 and B = 5.6 (McKeon, *et al.* 2004). A modified Clauser chart method, described by Perry & Li (1990), was employed to determine the friction velocity on the rough wall. Additional details of the experimental facilities and methods is found in Schultz and Flack (2007).

MEAN FLOW RESULTS

The mean velocity profiles for the rough-wall boundary layers in inner variables are shown in figure 3. The effect of increasing Reynolds number is seen as an increase in the

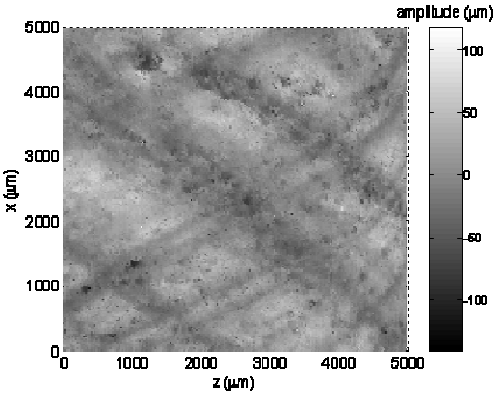

(a)

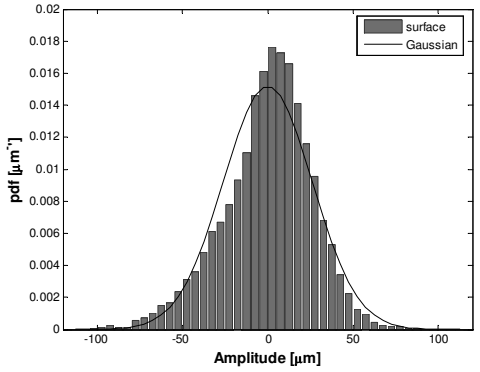

(b)

Figure 2. Test roughness: (a) surface elevation of roughness; (b) probability density function of roughness surface elevations.

downward shift in the overlap region of the profiles termed the roughness function, ΔU^+. Otherwise the profiles retain a similar shape. More effective comparisons of rough- and smooth-wall may be made with the mean profiles plotted in velocity-defect form. As is seen in figure 4, the agreement between the rough- and smooth-wall profiles is excellent. These mean flow results provide support for Townsend's (1976) Reynolds number similarity hypothesis and the proposal of a universal defect profile in the overlap and outer regions of the boundary layer for zero pressure gradient rough and smooth walls as proposed by Clauser (1954) and Hama (1954).

The roughness function results, ΔU^+, for the rough-wall profiles are presented in figure 5. Shown for comparison, are the rough-wall pipe flow results of Shockling, *et al.* (2006) that were obtained for a geometrically similar roughness. The agreement in the two data sets is excellent. It should be noted that both in the present boundary layer study and the pipe flow experiments of Shockling, *et al.* (2006), the relative roughness height or ratio of the roughness height to the thickness of the shear layer is much smaller than almost all previous roughness studies.

TURBULENCE RESULTS

Figure 7 shows the profiles of $\overline{u'^2}^+$ for the smooth and rough surfaces in outer scaling. Reynolds number dependence in the overlap region can be observed for both

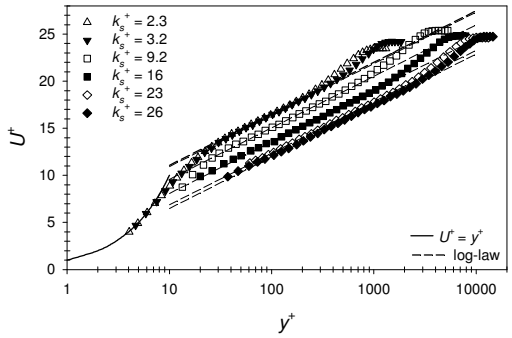

Figure 3. Rough-wall mean velocity profiles in inner variables, log constants of McKeon *et. al* (2004), uncertainty in U^+ ±4%.

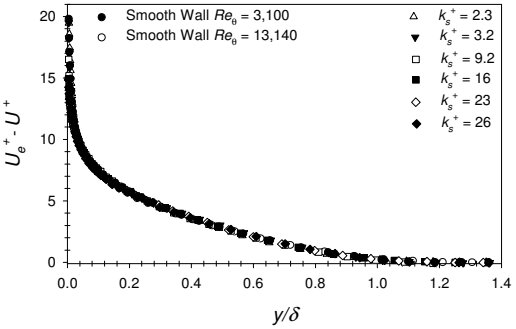

Figure 4. Mean velocity profiles in velocity-defect form for both smooth and rough walls, uncertainty in U_e^+-U^+ ±4%.

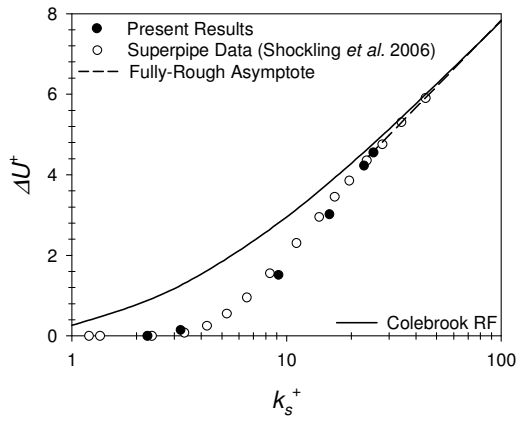

Figure 5. Roughness function results, ΔU^+ determined using the log constants of McKeon *et. al* (2004), uncertainty in ΔU^+ ±10% or 0.2, whichever is larger.

the smooth- and rough-wall cases. This is observed as a slight increase in $\overline{u'^2}^+$ with Reynolds number. There is, however, good agreement of the smooth- and rough-wall results in the overlap and outer region of the boundary layer when similar Reynolds number cases are compared. This similarity in the streamwise Reynolds normal stress for rough and smooth walls in the outer flow is fairly well accepted and has been observed in previous roughness studies (see the review articles of Raupach, *et al.* 1991 and Jiménez 2004). Likewise, the present streamwise Reynolds normal stress profiles provide support for the concept of wall similarity. It should also be noted that the present smooth-wall Reynolds stress profiles agree well with those of DeGraaff & Eaton (2000) at similar Reynolds numbers.

Figure 8 shows the profiles of $\overline{v'^2}^+$ for the smooth and rough surfaces in outer scaling. The agreement of the smooth and rough profiles is within the experimental uncertainty of the measurements across the overlap and outer regions of the boundary layer. For both the smooth- and rough-wall profiles, a rather broad plateau of $\overline{v'^2}^+ \approx 1.3$ – 1.4 is observed in the overlap region. This is in agreement with DeGraaff & Eaton (2000), who observed a plateau in $\overline{v'^2}^+ \approx 1.35$ for smooth walls at $Re_\theta \geq 2900$. The effect of roughness on the wall-normal or 'active' turbulent motions has been the topic of considerable debate. The research of Flack, *et al.* (2005) and Kunkel & Marusic (2006) support outer layer similarity while the research of Krogstad, *et al.* (1992) and Leonardi, *et al.* (2003) shows that roughness effects on the wall-normal component extend well into the outer layer. Jiménez (2004) tried to reconcile these conflicting views by concluding that the differences might be the effect of the relative roughness, k/δ, on the flow. The present $\overline{v'^2}^+$ profiles provide support for the concept of wall similarity for boundary layers in which the relative roughness is small and the Reynolds number is large.

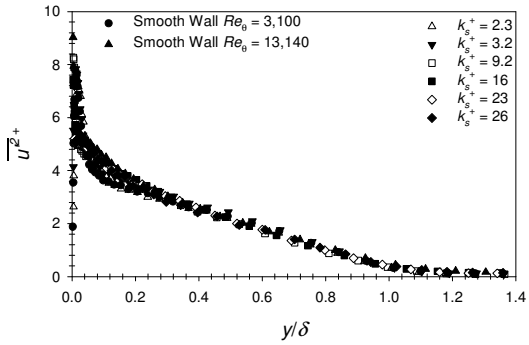

Figure 7. Streamwise Reynolds normal stress profiles in outer variables; uncertainty in $\overline{u'^2}^+$ ±8%.

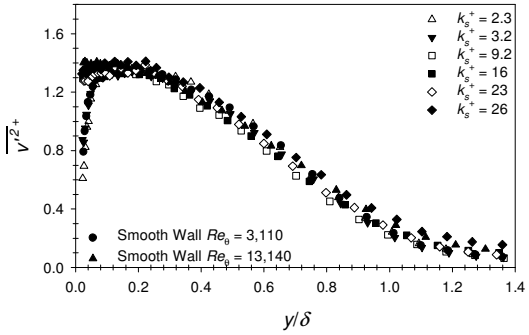

Figure 8. Wall-normal Reynolds normal stress profiles for all surfaces in outer scaling; uncertainty in $\overline{v'^2}^+$ ±9%.

The $-\overline{u'v'}^+$ profiles for the smooth and rough surfaces in outer scaling are shown in figure 9. Again, there is no significant difference in the smooth- and rough-wall profiles in the outer part of the boundary layer. Krogstad, *et al.* (1992) observed a moderate increase in $-\overline{u'v'}^+$ for a woven mesh roughness compared to a smooth wall in the outer layer. However, the difference was smaller than was seen

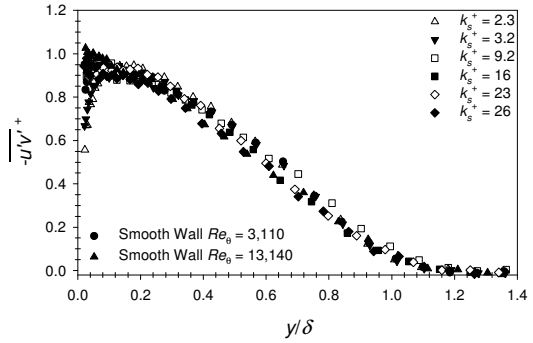

Figure 9. Reynolds shear stress profiles for all surfaces in outer scaling; uncertainty in $-\overline{u'v'}^+$ ±9%.

in $\overline{v'^2}^+$. The differences in $\overline{v'^2}^+$ and $-\overline{u'v'}^+$ were attributed in part to the less strict wall boundary condition for the wall-normal velocity component on a rough surface compared to a smooth one. However, the study of Flack, *et al.* (2005) found little change in the Reynolds stresses over woven mesh for $y > 3k_s$.

QUADRANT DECOMPOSITION

Quadrant decomposition (Wallace, *et al.* 1972) was used in order to examine possible changes in turbulence structure resulting from the honed surface roughness. The technique sorts turbulent events into each of the four quadrants of the (u', v') plane allowing the contributions of ejection (*Q*2) and sweep (*Q*4) motions to the total Reynolds shear stress to be calculated. In the present work, the quadrant decomposition was carried out using the hyperbolic hole size (*H*) method of Lu & Willmarth (1973).

Figures 10 and 11 show the percentage contributions from ejection and sweep events, respectively, to the Reynolds shear stress for $H = 0$. It should be noted that for clarity only the highest Reynolds number cases for the smooth and rough wall are presented for the quadrant decomposition. However, the trends were very similar for the lower Reynolds number cases.

The present results show that there is excellent agreement in the contributions from both *Q2* and *Q4* events for the smooth- and rough-wall boundary layers. This is in agreement with previous research by the present authors (Flack, *et al.* 2005) which showed similar results for both sandpaper and woven mesh roughness. The relative roughness height, k_s/δ, in that study was 1/62 and 1/45 for the sandpaper and mesh roughness, respectively. The ratio k_s/δ for the rough-wall results presented here is 1/400. In contrast, Krogstad, *et al.* (1992) observed a significant increase in $\left(-\overline{u'v'}\right)_2^+$ across much of the boundary layer for a woven mesh roughness compared to a smooth wall with *H*=0. An increase in $\left(-\overline{u'v'}\right)_4^+$ in the wall region was also noted. The ratio k_s/δ was 1/15 in that study. The differences observed among these studies may be a result of differences in scale separation between the roughness length scale and the largest turbulence scales in the flow.

Figures 12 and 13 show the percentage contributions from ejection and sweep events, respectively, to the conditionally averaged Reynolds shear stress for $H = 2$.

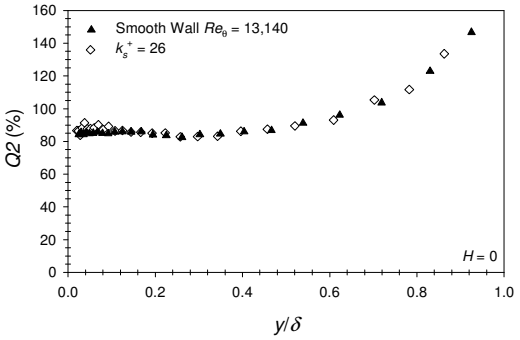

Figure 10. Percentage Contribution to the Reynolds shear stress from *Q2* events (*H*=0).

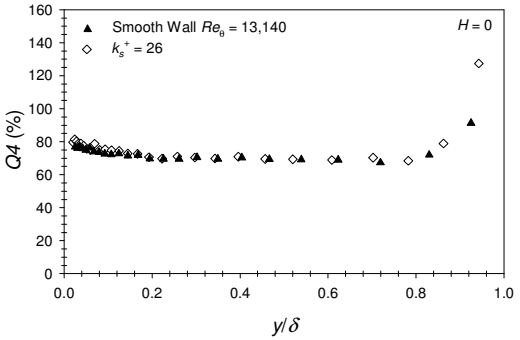

Figure 11. Percentage Contribution to the Reynolds shear stress from *Q4* events (*H*=0).

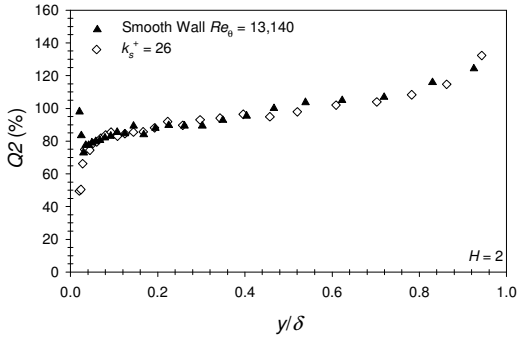

Figure 12. Percentage contribution to the conditionally averaged Reynolds shear stress from *Q2* events (*H*=2).

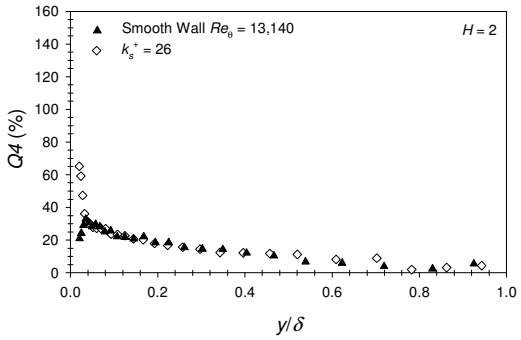

Figure 13. Percentage contribution to the conditionally averaged Reynolds shear stress from *Q4* events (*H*=2).

Using $H = 2$ isolates strong turbulence events in which the instantaneous Reynolds shear stress is larger in magnitude than $5\overline{u'v'}$. Again, the results show good agreement in the contributions from both *Q2* and *Q4* events for the smooth

boundary layer. However, near the wall ($y/\delta \leq 0.025$), the percentage contribution from strong ejection events on the rough wall decreases, while the percentage contribution from strong sweep events increases. In contrast, near the smooth wall, the contribution from strong ejection events increases, while the percentage contribution from strong sweep events decreases. These differences observed in the near-wall region between the rough and smooth walls are in agreement with the results of Krogstad, *et al.* (1992) and Flack, *et al.* (2005) for woven mesh, and sandpaper and woven mesh roughness, respectively. Krogstad & Antonia (1999) observed a similar trend for a transverse rod roughness with the effect persisting well into the outer flow. The relative roughness, k_s/δ was 1/8 in that study. In the present investigation in which the relative roughness is much smaller, the differences between the rough and smooth wall are confined to the near-wall region.

HIGHER ORDER STATISTICS

The velocity triple products will now be examined. As with the quadrant decomposition, only the highest Reynolds number cases for the smooth and rough wall are presented for the velocity triple products. Murlis, *et al.* (1982) noted that these quantities display only a weak Reynolds number dependence even at $Re_\theta < 5000$. For both the present cases shown, the Reynolds number is much higher ($Re_\theta > 13000$).

Profiles of the velocity triple product $\overline{u'^3}^+$ for the smooth and rough wall are shown in figure 14. Over most of the boundary layer the agreement between the rough and smooth wall is quite good. Near the wall at $y/\delta \leq 0.025$, some significant differences are noted. On the rough wall, $\overline{u'^3}^+$ changes sign and becomes positive near the roughness. For the smooth wall, it remains negative across the entire boundary layer.

The distributions of the velocity triple product $\overline{v'^3}^+$ are presented in figure 15. The present smooth- and rough-wall results agree within their uncertainty throughout the boundary layer. Antonia & Krogstad (2001) showed that the profile of $\overline{v'^3}^+$ was considerably altered for flows over transverse rods. They observed that the value of $\overline{v'^3}^+$ was negative over a significant fraction of the boundary layer while this triple product remained positive for a smooth and a woven mesh roughness over the entire layer. It is not clear if the differences observed are due fundamental differences in the flows over two- and three-dimensional roughness. Bandyopadhyay & Watson (1988) observed similar differences in the velocity triple products between two- and three-dimensional roughness.

The results for the velocity triple product $\overline{u'^2 v'}^+$ are shown in figure 16. This term represents the wall-normal transport of the u'^2 contribution to the *TKE* by the v' fluctuations. The present results show good similarity in $\overline{u'^2 v'}^+$ for smooth and rough walls in the outer flow. Closer to the wall the results are a bit more scattered, but the differences observed are within the experimental uncertainty of the measurements.

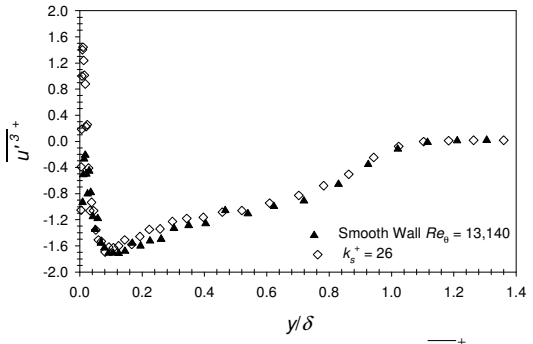

Figure 14. The velocity triple product $\overline{u'^3}^+$ for highest Reynolds number smooth and rough walls in outer scaling; uncertainty in $\overline{u'^3}^+$ ±16%.

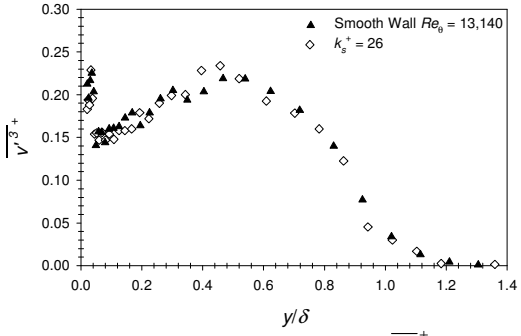

Figure 15. The velocity triple product $\overline{v'^3}^+$ for highest Reynolds number smooth and rough walls in outer scaling; uncertainty in $\overline{v'^3}^+$ ±25%.

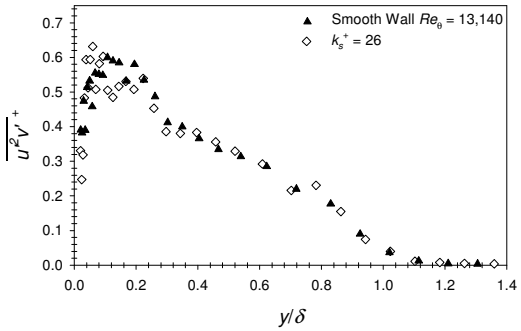

Figure 16. The velocity triple product $\overline{u'^2 v'}^+$ for highest Reynolds number smooth and rough walls in outer scaling; uncertainty in $\overline{u'^2 v'}^+$ ±17%.

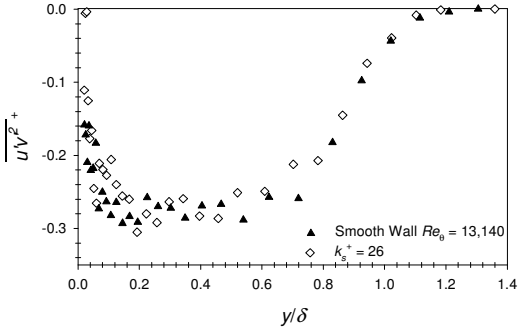

Figure 17. The velocity triple product $\overline{u'v'^2}^+$ for highest Reynolds number smooth and rough walls in outer scaling; uncertainty in $\overline{u'v'^2}^+$ ±19%.

The profiles of the velocity triple product $\overline{u'v'^2}^+$ are shown in figure 17. This triple product represents the wall-normal turbulent flux of the Reynolds shear stress. Although there is some scatter in the present results, there are no striking differences observed between the smooth- and rough-wall profiles over most of the boundary layer. Previous research by the present authors (Flack, *et al.* 2005) also showed good agreement in $\overline{u'v'^2}^+$ for rough- and smooth-wall boundary layers over much of the boundary layer. However, for both the sandpaper and woven mesh roughness that were tested, $\overline{u'v'^2}^+$ became positive near the wall ($y < 5k_s$), indicating a flux of Reynolds shear stress toward the surface as opposed to away from it, as is observed here. This change in near-wall transport was also noted by Andreopoulos & Bradshaw (1981).

CONCLUSIONS

Measurements that cover a wide Reynolds number range, spanning the hydraulically smooth to the fully rough flow regime for a single surface with a small relative roughness height, have been presented and compared to those for a smooth wall. The roughness functions (ΔU^+) show good agreement with the Superpipe results of Shockling, *et al.* (2006) and indicate that a three-dimensional roughness with a nearly Gaussian distribution shows inflectional behavior, not following a monotonic, Colebrook-type roughness function (Colebrook 1939) as suggested by the Moody diagram (1944).

The present results for the mean flow, Reynolds stresses, quadrant decomposition of the Reynolds shear stress, and velocity triple products all show excellent agreement between rough- and smooth-wall boundary layers in the overlap and outer regions, and, therefore, provide compelling support for the wall similarity hypothesis. These results indicate that if the separation of scales between roughness and largest turbulent length scales is sufficient, the outer layer is independent of surface condition except for the role that the wall conditions have on setting the length (δ) and velocity (U_τ) boundary conditions for the outer flow.

The authors would like to acknowledge the financial support or the Office of Naval Research for this project.

REFERENCES

Andreopoulos, J. & Bradshaw, P. 1981 Measurements of turbulence structure in the boundary layer on a rough surface. *Boundary-Layer Meteorology* **20**, 201-213.

Antonia, R.A. & Krogstad, P.-Å. 2001 Turbulence structure in boundary layers over different types of surface roughness. *Fluid Dyn. Res.* **28**, 139-157.

Bandyopadhyay, P.R. & Watson, R.D. 1988 Structure of rough-wall boundary layers. *Phys. Fluids* **31** 1877-1883.

Bhaganagar, K., Kim, J., & Coleman, G. 2004 Effect of roughness on wall-bounded turbulence. *Flow Turbulence and Combustion* **72**, 463-492.

Clauser, F.H. 1954 Turbulent boundary layers in adverse pressure gradients. *J. of the Aero. Sci.* **21**, 91-108.

Colebrook, C.F. 1939 Turbulent flow in pipes, with particular reference to the transitional region between smooth and rough wall laws. *J. of Inst. of Civil Engrs.* **11**, 133-156.

DeGraaff, D.B. & Eaton J.K. 2000 Reynolds-number scaling of the flat-plate turbulent boundary layer. *J. Fluid Mech.* **422**, 319-346.

Flack, K.A., Schultz, M.P., & Shapiro, T.A. 2005 Experimental support for Townsend's Reynolds number similarity hypothesis on rough walls. *Phys.Fluids* **17**: #035102.

Hama, F.R. 1954 Boundary-layer characteristics for rough and smooth surfaces. *Trans. SNAME* **62**, 333-351.

Jiménez, J. 2004 Turbulent flows over rough walls. *Ann. Rev. of Fluid Mech.* **36**, 173-196.

Keirsbulck, L., Labraga, L., Mazouz, A., & Tournier, C. 2002 Surface roughness effects on turbulent boundary layer structures. *J. Fluids Engr.* **124**, 127-135.

Krogstad, P.-Å. & Antonia, R.A. 1999 Surface roughness effects in turbulent boundary layers. *Experiments in Fluids* **27**, 450-460.

Krogstad, P.-Å., Antonia, R.A., & Browne, L.W.B. 1992 Comparison between rough- and smooth-wall turbulent boundary layers. *J. Fluid Mech.* **245**, 599-617.

Kunkel, G.J. & Marusic, I. 2006 Study of the near-wall-turbulent region of the high-Reynolds-number boundary layer using an atmospheric flow. *J. Fluid Mech.***548**, 375-402.

Leonardi, S., Orlandi, P., Smalley, R.J., Djenidi, L., & Antonia, R.A. 2003 Direct numerical simulations of turbulent channel flow with transverse square bars on one wall. *J. Fluid Mech.* **491**, 229-238.

Lu, S.S. & Willmarth, W.W. 1973 Measurements of the structure of the Reynolds stress in a turbulent boundary layer. *J. Fluid Mech.* **60**, 481-571.

McKeon, B.J., Li, J., Jiang, W., Morrison, J.F., & Smits, A.J. 2004 Further observations on the mean velocity distribution in fully developed pipe flow. *J. Fluid Mech.* **501**, 135-147.

Moody, L.F. 1944 Friction factors for pipe flow. *Trans. A.S.M.E.* **66**, 671-684.

Murlis, J., Tsai, H.M., & Bradshaw, P. 1982 The structure of turbulent boundary layers at low Reynolds numbers. *J. Fluid Mech.* **122**, 13-56.

Perry, A.E. & Li, J.D. 1990 Experimental support for the attached-eddy hypothesis in zero-pressure gradient turbulent boundary layers. *J. Fluid Mech.* **218**, 405-438.

Raupach, M.R., Antonia, R.A., & Rajagopalan, S. 1991 Rough-wall boundary layers. *Applied Mech. Rev.* **44**, 1-25.

Schultz, M.P & Flack, K.A. (2007) The rough-wall turbulent boundary layer from the hydraulically smooth to the fully rough regime. *J. Fluid Mech.* **580**, 381-405.

Shockling, M.A., Allen J.J., & Smits, A.J. 2006 Roughness effects in turbulent pipe flow. *J. Fluid Mech.***564**, 267.

Tachie, M.F., Bergstrom, D.J., & Balachandar, R. 2000 Rough wall turbulent boundary layers in shallow open channel flow. *J. Fluids Engr.* **122**, 533-541.

Townsend, A.A. 1976 *The Structure of Turbulent Shear Flow*. 2nd Edition, Cambridge University Press.

Wallace, J.M., Eckelmann, H., & Brodkey, R.S. 1972 The wall region in turbulent shear flow. *J. Fluid Mech.* **54**, 39-48.